

Deep-mixing and deep-cooling events in Lake Garda: Simulation and mechanisms

Bouke Biemond,^{1*} Marina Amadori,^{2,3} Marco Toffolon,² Sebastiano Piccolroaz,⁴
Hans van Haren,⁵ Henk A. Dijkstra¹

¹Institute for Marine and Atmospheric research Utrecht, Department of Physics, Utrecht University, the Netherlands

²Department of Civil, Environmental and Mechanical Engineering, University of Trento, Italy

³Institute for Electromagnetic Sensing of the Environment, National Research Council, Milan, Italy

⁴Physics of Aquatic Systems Laboratory (APHYS) - Margaretha Kamprad Chair, École Polytechnique Fédérale de Lausanne, Switzerland

⁵Royal Netherlands Institute for Sea Research (NIOZ), the Netherlands

*Corresponding author: w.t.biemond@uu.nl

1. Analysis of a thermocline tilting event

In Fig. S1, the simulated water temperature, velocities and ε are displayed during a thermocline tilting event. Along the main axis of the lake (Fig. S1a-b, Fig. 7a) warm surface water flows to the south and cold bottom water flows to the north because of strong southward winds. In the subsequent days, vertical thermal stratification disappears almost completely (Fig. S1c-d, Fig. 7b). When the wind weakens (at day 30), the water starts to flow back to its previous position (Fig. S1e-f, Fig. 7c). The development of this wind-driven basin scale flow causes a spike in the deep water temperature signal, because warm water reaches the bottom (Fig. S1c) but disappears a few days later (Fig. S1g-h) again (when the wind weakens and the stratification recovers). The (short-living and local) disappearance of stratification in combination with strong winds causes mixing over the entire water column, observed for example in Fig. S1d, giving a DME. Some cooling of the surface waters by the wind during this event will decrease the bottom water temperature slightly (Fig. S1e), but not sufficiently to cause a DCE.

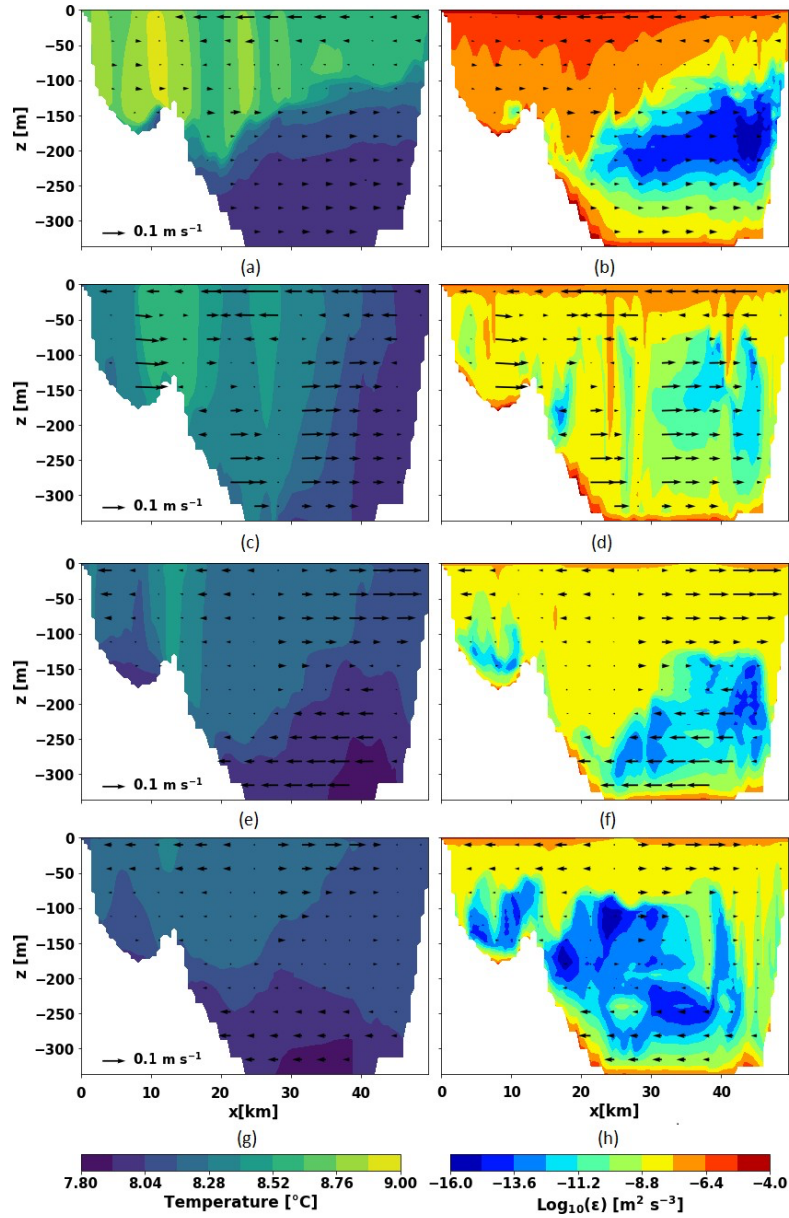


Fig. S1. Transects of temperature, velocities (vectors) and turbulent kinetic energy dissipation rate (ϵ) from the Delft3D simulation for specific date times in 2005. The transect is taken along the red line in Fig 1. (a) Transect of temperature on day 24 (time=10:00 UTC). (b) As (a), but for ϵ . (c)-(d) as (a)-(b), but on day 27. (e)-(f) as (a)-(b), but on day 32. (g)-(h) as (a)-(b), but on day 36.

2. Analysis of a turbulent cooling event

Fig. S2 shows turbulent cooling simulated in 2005 at ARPAV1 and reveals that strong wind speeds (Fig. S2a) and a strong negative surface heat flux (Fig. S2b) are present while in the meantime the air temperature is below the freezing point (Fig. S2c). Shortly after the offset of the strong wind, stratification disappears completely (Fig. S2d) and turbulence reaches the bottom (Fig. S2f) since there is no stratification to prevent this. The entire water column thus cools during this process, because of the full vertical extent of the mixing and the low surface heat flux. Significant vertical velocities are present during turbulent cooling events (Fig. S2e). This is a signature of convection as cold water from the surface sinks to the bottom. Both terms P_k and B_k of buoyancy and shear induced TKE production are displayed in Fig. S2g and Fig. S2h, respectively. Both peak at the surface and decrease when going downwards. Production of TKE by shear dominates over buoyancy when averaging (indicated by quantities with a bar) over the entire water column and over day 57.5-59.5 ($\bar{P}_k = 1.66 \times 10^{-7} \text{ m}^2 \text{ s}^{-3}$ and $\bar{B}_k = 0.389 \times 10^{-7} \text{ m}^2 \text{ s}^{-3}$) and also in the bottom 150 m ($\bar{P}_k = 1.49 \times 10^{-8} \text{ m}^2 \text{ s}^{-3}$ and $\bar{B}_k = 1.11 \times 10^{-8} \text{ m}^2 \text{ s}^{-3}$). This means that the effect of wind stress (as the major source of horizontal shear) on turbulence production dominates here over surface cooling. However, this ratio varies for different events. The median values over the entire column ($\bar{P}_k = 1.61 \times 10^{-8} \text{ m}^2 \text{ s}^{-3}$ and $\bar{B}_k = 1.92 \times 10^{-8} \text{ m}^2 \text{ s}^{-3}$) and for the bottom 150 m ($\bar{P}_k = 3.39 \times 10^{-9} \text{ m}^2 \text{ s}^{-3}$ and $\bar{B}_k = -9.12 \times 10^{-12} \text{ m}^2 \text{ s}^{-3}$) provide a different view as the average values mentioned earlier are dominated by large values. However, the picture from the median is not necessarily better as the large values are more important for assessing the dominance of one mechanism over another.

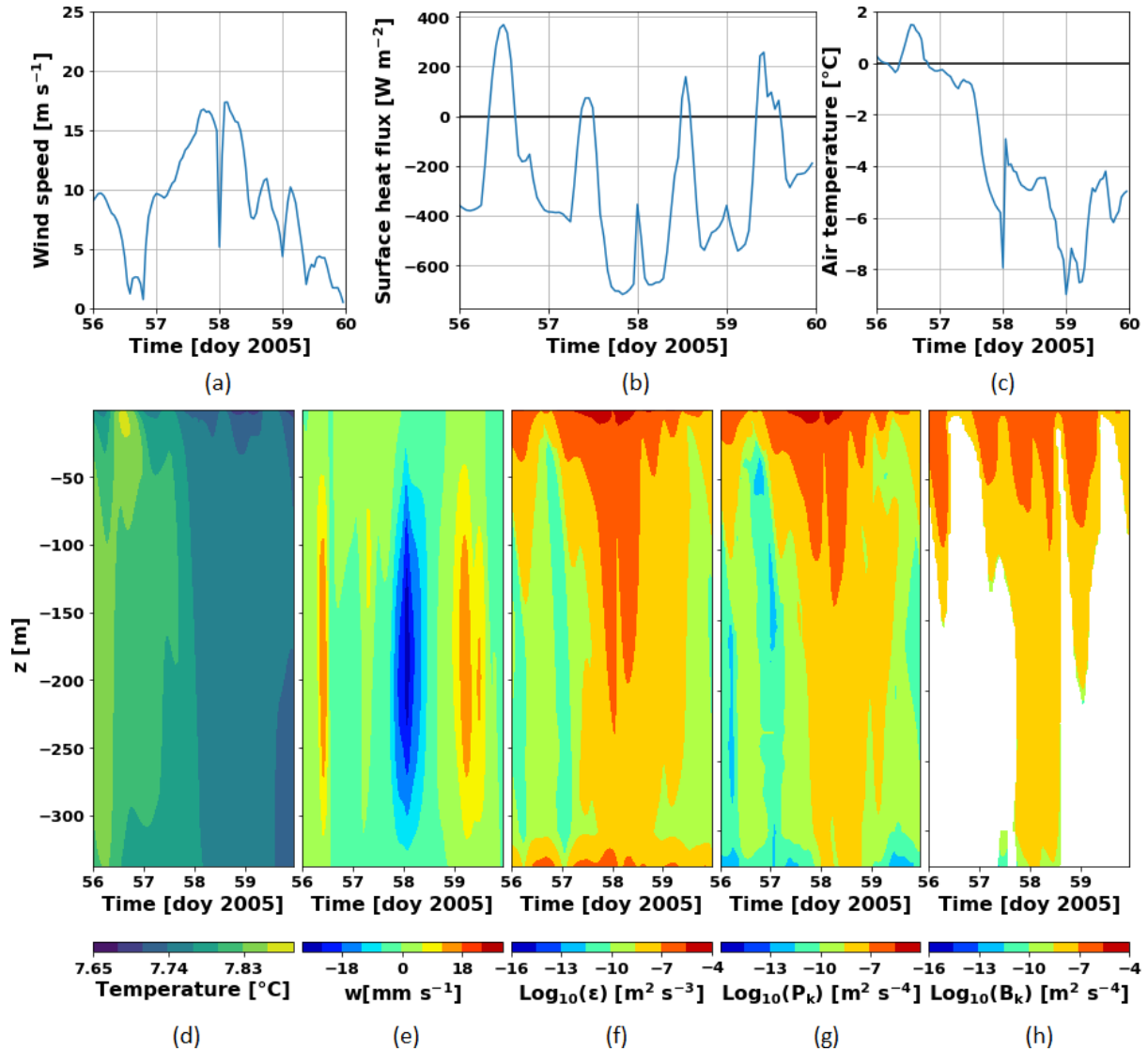


Fig. S2. Variables during a turbulent cooling event in 2005 at the ARPAV1 point. Data from the Delft3D and WRF simulation. (a) Wind speed versus time. (b) Surface heat flux *versus* time. (c) Air temperature *versus* time. Plots of different variables *versus* time and vertical coordinate: (d) water temperature; (e) vertical velocity component; (f) TKE dissipation rate (ϵ); (g) production of TKE by shear; (h) production of TKE by buoyancy. The white area is where the production is negative. The spike at doy 58 is due to a restart of the WRF simulation.

3. Analysis of a differential cooling event

A simulated turbulent cooling event is visible in Fig. S3a-b, again in the winter of 2005; here turbulence is strong over the whole lake, and cooling occurs over the entire water column (Fig. 7j). There is some stratification visible in the southern part of the lake and turbulent cooling does not reach the bottom there at this time. In Fig. S3c-d, turbulence has ceased in the deep parts of the lake, but deep-water cooling is visible, which is confirmed by Fig. S3e-f, where the bottom layer clearly has cooled since day 64 (Fig. 7l). This cold water cannot be created by turbulent cooling at that location, since the surface water never was this cold. Instead, the origin of the cold water is advection of water from the shallower parts of the lake, through bottom currents (Fig. 7k). This is confirmed by the currents in the model, where a northward current is present close to the bottom (Fig. S3c-f). The spread of the cold water matches with the along-channel bottom flow velocities. The flow simulated during these events is independent of wind speed and direction at that time, and differential cooling happens even when the wind is very weak. The northward bottom currents are caused by density differences: cold water from the south flows to the deep northern part because of its larger density. The simulation shows that it takes approximately one week to reach the north. In this way, differential cooling generates stratification in the deep part of the lake because cold water flows beneath warm water (Fig. 7l). Fig. S4 confirms that the cooling taking place in 2005 was due to this mechanism, since bottom temperature at the (shallow) ARPAV2 point is lower than that at the (deep) ARPAV1 point. This creates the situation required for bottom water cooling in the deep part by advection. Inspecting the temperature profile at the ARPAV1 point in Fig. S4, it is visible that just above the bottom cold water is present over a small depth range. This signature could be used to distinguish future DCEs, as it should be visible in temperature time series at different depths.

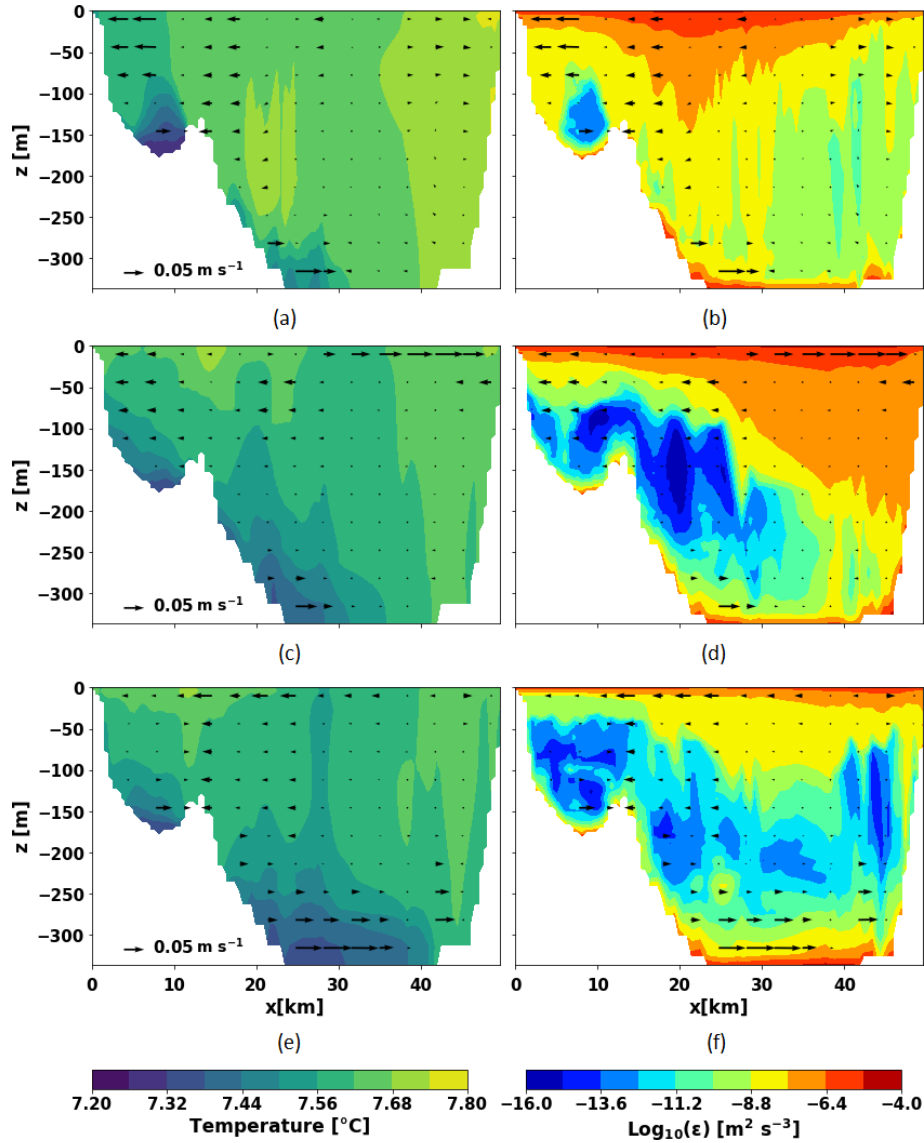


Fig. S3. Transects of temperature, velocities (vectors) and TKE dissipation rate (ϵ) from the Delft3D simulation for specific date times in 2005. The transect is taken along the red line in Fig. 1. (a) Transect of T on day 64 (time=10:00 UTC). (b) As (a), but for ϵ . (c)-(d) as (a)-(b), but on day 70. (e)-(f) as (a)-(b), but on day 72.

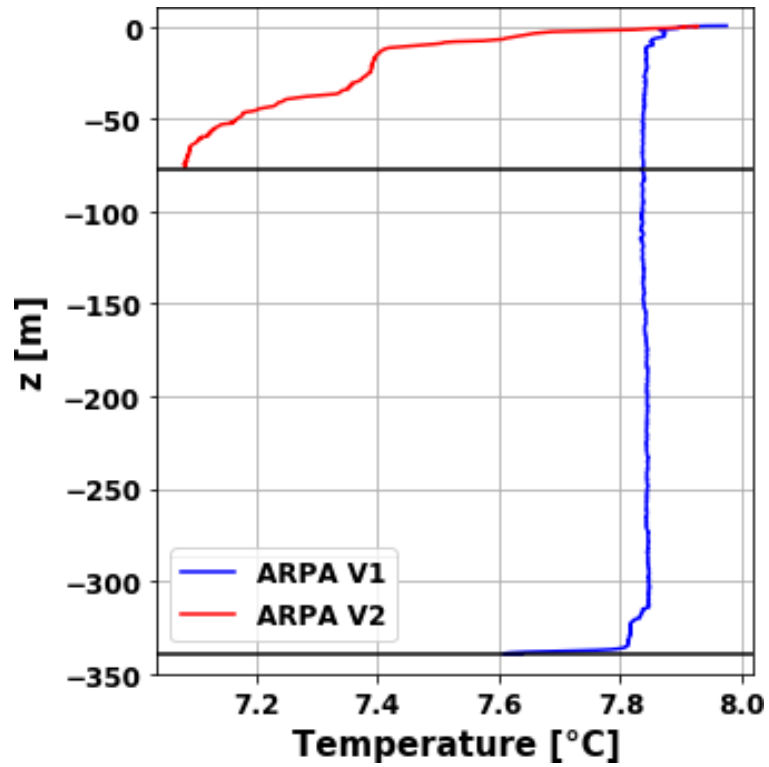


Fig. S4. Temperature profiles at the ARPAV1 and ARPAV2 points, observed on day 66 of 2005. The blue line represents the ARPAV1 point and the red line the ARPAV2 point. The horizontal black lines are the respective depths.